



Research article

Potential of pre-interventional magnetic resonance angiography for optimization of workflow and clinical outcome of prostatic arterial embolization

Thomas J. Vogl^{a, 1}, Christian Booz^{a, b, 1}, Vitali Koch^{a, b}, Nour Eldin A. Nour-Eldin^{a, c}, Emad H. Emara^d, Felix Chun^e, Shirin El Nemr^{a, b}, Leona S. Alizadeh^{a, b, *}

^a Department of Diagnostic and Interventional Radiology, University Hospital Frankfurt, Germany

^b Division of Experimental Imaging, Department of Diagnostic and Interventional Radiology, University Hospital Frankfurt, Germany

^c Department of Diagnostic and Interventional Radiology, University Hospital Cairo, Egypt

^d Department of Diagnostic and Interventional Radiology, Kafrelsheikh University, Egypt

^e Department of Urology, University Hospital Frankfurt, Germany

ARTICLE INFO

Keywords:

Prostatic artery embolization

MRA

Lower urinary tract symptoms

Prostatic hyperplasia

Workflow

ABSTRACT

Purpose: Impact of pre-interventional magnetic resonance angiography (MRA) on prostatic artery embolization (PAE) regarding workflow, radiation dose, and clinical outcome.

Method: Retrospective evaluation of 259 patients (mean age 68 ± 9 , range 41–92) with benign prostatic hypertrophy (BPH) undergoing PAE between January 2017 and December 2020. MRA was performed in 137 cases. In 122 patients, no pre-interventional MRA was performed. Origin of the PA, volumetry of the prostatic gland and ADC values were evaluated. International Prostate Symptom Score (IPSS), Quality of Life (QoL) and International Index of Erectile Function (IIEF) were evaluated before and after PAE.

Results: Origin of the PA was identified in all cases. Significant differences regarding volume reduction (-20 ± 13 ml with MRA vs -17 ± 9 ml without MRA) and ADC value reduction were found ($-78 \pm 111 \cdot 10^{-6}$ mm²/s with MRA vs $-45 \pm 99 \cdot 10^{-6}$ mm²/s without MRA). PAE workflow was modified in 16 patients due to MRA findings. Radiation dose (5518.54 ± 6677.97 μGym² with MRA vs 23963.50 ± 19792.25 μGym² without MRA) and fluoroscopy times (19.35 ± 9.01 min. with MRA vs 27.45 ± 12.54 min. without MRA) significantly differed. IPSS reduction improved (-11 ± 8 points with MRA vs -7 ± 9 points without MRA, $p < 0.001$), while QoL (-2 ± 1 points with MRA and -2 ± 2 points without MRA) and IIEF ($+2 \pm 10$ points with MRA and $+1 \pm 11$ points without MRA) showed no significant differences ($p > 0.05$).

Conclusions: Pre-interventional MRA facilitates improved workflow and patient safety of PAE while reducing radiation dose and intervention time.

1. Introduction

Prostate artery embolization (PAE) is an increasingly performed, internationally accepted yet controversially discussed minimally invasive therapy option for patients with benign prostate hyperplasia (BPH) [1, 2].

Despite being considered safe and effective, PAE represents one of the most challenging procedures in interventional radiology [3,4]. For image guidance during PAE, fluoroscopy and digital subtraction angiography (DSA) are used. Long procedure and examination times lead to peaks in cumulative radiation exposure for patients and medical staff [5]. Deterministic tissue damage, such as radiation erythema and hair-

Abbreviations: BPH, Benign prostatic hyperplasia; BPS, Benign prostatic syndrome; CBCT, Cone Beam Computed Tomography; DAP, Dose area product; DSA, Digital subtraction angiography; IPSS, International Prostate Symptom Score; IIEF, International Index of Erectile Function; LUTS, Lower urinary tract symptoms; MIP, Maximum intensity projection; MRA, Magnetic resonance angiography; PA, Prostate artery; PAE, Prostatic artery embolization; PSA, Prostate-specific antigen; PV, Prostate volume; QoL, Quality of life; RP, Air kerma; SR, Structured report; VRT, Volume Rendering Technique

* Corresponding author at: University Hospital Frankfurt, Department of Diagnostic and Interventional Radiology, Theodor-Stern-Kai 7, 60590 Frankfurt, Germany.

E-mail address: leona.alizadeh@outlook.de (L.S. Alizadeh).

¹ Shared first authorship.

<https://doi.org/10.1016/j.ejrad.2022.110236>

Received 21 December 2021; Received in revised form 27 January 2022; Accepted 3 March 2022

0720-0488/© 20XX

loss may occur from a cumulative dose of 500 mSv upwards [6], which can be reached during PAE. Additionally, late onset stochastic cell damage (cancer) increases with every mSv of radiation exposure to staff and patients [5]. In this context, detailed knowledge of the individual vascular anatomy, which shows great variability between patients, is very important [7]. Pre-interventional imaging is used to reduce radiation dose, improve workflow, patient safety and outcome. Currently, pre-procedural computed tomography angiography (CTA) [8] and/or intra-procedural cone beam CT (CBCT)-angiography are used to visualize the vascular anatomy [9], resulting in additional effective dose for patients [5,10]. Pre-interventional high-resolution magnetic resonance angiography (MRA) may be a valuable alternative to CTA and CBCT without causing additional radiation exposure [11,12]. Pre-interventional MRA significantly reduces radiation dose and improves clinical outcome (Zhang et al.) [11]. However, no studies to date have evaluated the direct influence of pre-interventional MRA on PAE workflow, clinical outcome as well as ADC value reduction. We aimed to compare PAE procedures in patients who had undergone pre-interventional MRA and patients without pre-interventional imaging regarding prostate volumetry changes, clinical outcome, radiation dose and potential for PAE workflow optimization.

2. Material and methods

2.1. Patient inclusion

This retrospective study was approved by the local institutional ethics committee. Informed consent was waived. Multi-parametric MRI for ruling out malignancy was mandatory. Thus, only patients with prostate imaging reporting and data system (Pi-RADS-2) multi-parametric MRI [13,14] scores of 0–2, that did not show features of malignancy and negative PSA-values in a blood test ($\text{PSA} < 4 \text{ ng/ml}$ or increment of PSA per anno $< 0.35 \text{ ng/ml}$ [15]) were included to rule out malignant reasons for hyperplasia of the prostatic gland.

266 patients with severe lower urinary tract symptoms (LUTS) [16] and BPH that were refractory to conservative medical treatment who had undergone PAE at our institution between January 2017 and December 2020 were screened for study enrollment. 7 patients were excluded according to the following exclusion criteria: missing IPSS ($n = 4$), QoL ($n = 1$), IIEF ($n = 2$) before or after PAE treatment; history of biopsy-proven prostate cancer (see STARD-statement Fig. 1).

The final study population consisted of 259 patients. Patient characteristics are summarized in Table 1.

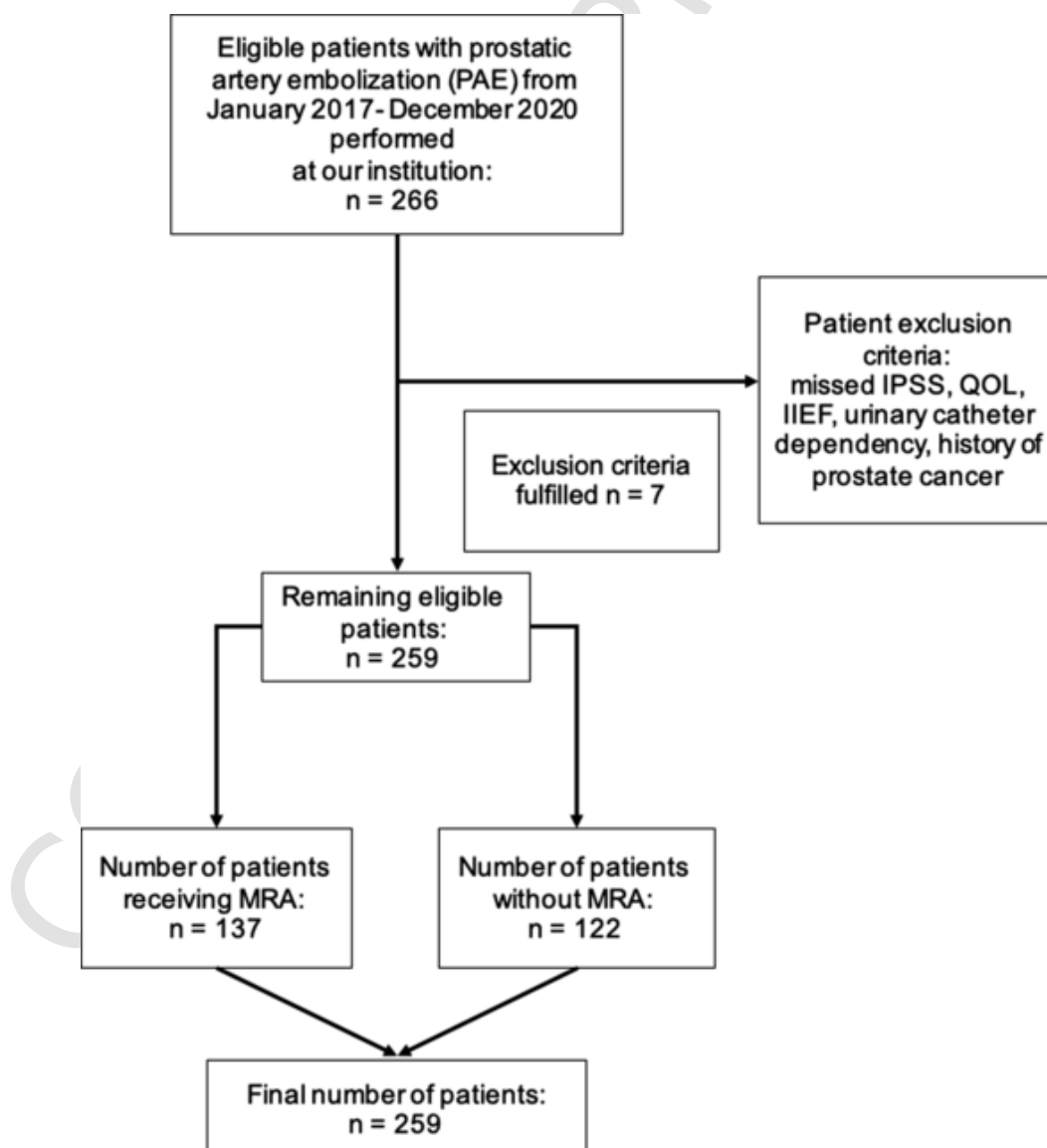


Fig. 1. Flow chart displaying the selection process in this study. LUTS, lower urinary tract symptoms; PAE, prostate artery embolization; MRI magnetic resonance imaging; IPSS, international prostate symptom score; QoL, quality of life; IIEF, international index of erectile function.

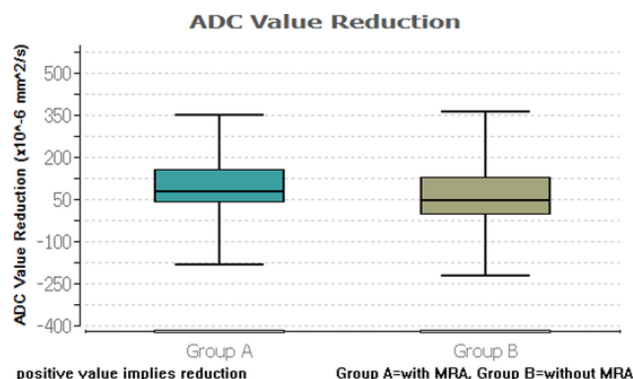


Fig. 2. Boxplot comparing apparent diffusion coefficient (ADC) value reduction in follow up magnetic resonance imaging (MRI) between Group A and Group B. Group A showed significantly higher reduction of ADC values between pre- and postinterventional MRI acquisitions.

Table 1

Patient demographics. N number of patients. Values are mean \pm standard deviation (range); $p < 0.05$ indicates a significant difference between Group A and Group B. IPSS, international prostate symptom score; QoL, quality of life; IIEF, international index of erectile function; PAE, prostate artery embolization; PV prostate volume.

	GROUP A	GROUP B	
	MRA prior to PAE (n = 137)	No imaging prior to PAE (n = 122)	P-value
Age, y	68.00 (± 8.86 ; 41–87)	69.00 (± 8.44 ; 49–92)	0.54
PSA [ng/ml]	1.8 (± 0.09 ; 0.01–2.1)	2.0 (± 1.2 ; 0.03–1.9)	0.26
IPSS score (possible range 0–35)			
pre-PAE	20.74 (± 7.00 ; 17–34)	20.75 (± 6.44 ; 16–35)	0.57
post-PAE	10.24 (± 8.24 ; 5–18)	13.75 (± 8.50 ; 6–16)	0.29
p	< 0.001	< 0.001	
QoL score (possible range 0–5)			
pre-PAE	4.06 (± 1.29 ; 3–5)	4.12 (± 1.21 2–5)	0.13
post-PAE	2.13 (± 1.32 1–4)	2.20 (± 1.50 1–4)	0.17
p	< 0.001	< 0.001	
IIEF (possible range 1–30)			
pre-PAE	21.50 (± 10.15 ; 9–28)	23 (± 11.32 ; 8–29)	0.41
post-PAE	24.00 (± 10.38 ; 9–28)	24 (± 11.03 ; 8–29)	0.29
p	0.216	0.332	
PV, [ml]			
pre-PAE	75.43 (± 49.12)	71.68 (± 31.18)	0.25
post-PAE	55.51 (± 13.22)	54.83 (± 32.27)	0.27
p	0.032	0.034	

2.2. Pre-interventional MRA

Pre-interventional MRI including contrast-enhanced MRA was performed with a 3.0-Tesla MRI system (MAGNETOM Prisma; Siemens Healthineers, Forchheim, Germany) and a body array coil. Gradient-echo scout images (repetition time msec/echo time msec, 6.9/3.75; flip angle, 35°; section thickness, 8 mm; matrix, 192/256; field of view (FOV), 45 cm) as well as T2-weighted single-shot turbo spin-echo MR images (repetition time msec/echo time msec 7500/100; flip angle, 160°; section thickness, 3.5 mm; matrix, 320/320; voxel dimensions, 0.6/0.6/3.5 mm; FOV, 20 cm) were performed in the axial, coronal, and sagittal direction. An unenhanced 3D fast low-angle shot sequence (repetition time msec/echo time msec 3.1/1.12; flip angle, 30°; section thickness, 0.9 mm; matrix, 312/416; FOV, 38 cm; voxel dimensions, 0.9/0.9/0.9 mm) was obtained before conducting the contrast-enhanced MR angiography with a 3D fast low-angle shot sequence (repetition time msec/echo time msec 3.1/1.12; flip angle, 30°; section thickness, 0.9 mm; matrix, 312/416; FOV 38 cm; voxel dimensions,

0.9/0.9/0.9 mm) in the arterial and venous phases. For determining contrast medium travel time, a test bolus was applied. MRA was performed with 1.5 ml/sec of 0.1 ml/kg of gadobutrol (Gadovist; Bayer Vital GmbH, Leverkusen, Germany) [17].

2.3. MRA image reconstruction and evaluation

Subtracted images were used to create maximum-intensity projection (MIP) reconstructions and a coloured three-dimensional free-rotatable, volume-rendered model of pelvic arteries (syngo.via®; Siemens Healthineers, Forchheim, Germany). 3D reconstruction volume rendering technique (VRT) was utilized to detect the optimal C-arm obliquity angle and to visualize origin and course of PA as well as vascular variants or pathologies such as stenosis prior to PAE [4,7,18]. MIP and VRT reconstructions of contrast enhanced MRA were displayed as a reference in the angiography room during the intervention to visualize pelvic arteries and identify target vessel. All MRA images were analyzed by two board-certified radiologists, *BLINDED* and *BLINDED*, with over 6 and 30 years of experience in urogenital MRI in consensus reading sessions. PA origin classification by de Assis et al. was used [18]: from superior vesical artery from the anterior trunk of internal iliac artery (type I); from anterior trunk of internal iliac artery, distal to superior vesical artery (gluteal pudendal trunk; type II); from obturator artery (type III); from internal pudendal artery (type IV); from other origins (type V).

Initial and post-embolization volumetry of the prostate was performed based on analysis of axial and sagittal T2w sequences and calculated with axial, anterior-posterior and craniocaudal diameter ((height \times width \times length) \times 0.52 formula) as described by Sosna et al. [19]. Furthermore, all patients were initially evaluated according to Pi-RADS-2 to rule out prostatic cancer.

2.4. Evaluation of ADC values from pre-interventional MP-MRI

Multiparametric pre- and post-interventional MRI were analysed for ADC reduction. ADC maps were derived from diffusion weighted imaging (DWI) sequences (500, 1500 DWIF) from the pre-interventional MP-MRI (acquired within 1 week prior to embolization) and in the follow-up MP-MRI within 4–6 weeks after PAE. ADC maps were assessed by the experienced board-certified radiologist *BLINDED* with more than 6 years of experience in reporting pelvic MRI, using 5–10 regions of interest (ROIs) measuring ADC values of the prostatic gland parenchyma. Measurements were repeated in accordance with the pre-interventional measurements in the follow-up MP-MRI. The final ADC value was the average of the values acquired of three local measurements.

2.5. PAE procedure

PAE was performed on a latest generation angiography suite (ARTIS pheno®; Siemens Healthineers, Forchheim, Germany). PERfectED technique (Carnevale et. al) was applied [20]. Standard protocol consisted in a right-sided transfemoral access. After femoral puncture, or if femoral access was not possible from either side a transbrachial puncture, a 5F sheath was introduced at the discretion of the interventional radiologist (*BLINDED*) with more than 25 years of experience in interventional radiology. Standard catheters (Sidewinder, Pigtail, Cobra) as well as 2.4F microcatheters (Progreat; Terumo, Tokyo, Japan) were introduced. Embolization was performed using either 100–300 μ m or 300–500 μ m microspheres (Embosphere® Microspheres; ©2018 Merit Medical Systems, South Jordan, Utah, USA). In all cases bilateral treatment was performed.

2.6. PAE workflow evaluation

Interventional access sites, amount of contrast agent, as well as used catheter types were noted for each PAE intervention. Modifications of standard PAE procedure protocol were recorded. Major and minor complications such as aneurysm, dissection, bleeding, misembolization, interruption of treatment etc. were recorded.

2.7. Radiation dose

For radiation dose evaluation the SR-files of all angiographic interventions were analyzed regarding dose area product (DAP) and air-kerma (RP). In addition, fluoroscopy time, as well as number of acquired DSA series were reported from SR-files.

2.8. Clinical outcome assessment

Clinical outcome was assessed by comparing the following aspects prior and after interventions: Erectile dysfunction was evaluated using the International Index of Erectile Function (IIEF) [21]. Quality of Life-Score was examined (QoL, ranging from 0 [delighted] to 6 [terrible]). LUTS were determined using the International Prostate Symptom Score (IPSS) questionnaire [22]. The questionnaire includes 7 questions regarding BPH symptoms: urination frequency, nocturia, weak urinary stream, hesitancy, intermittence, incomplete emptying of the bladder and urinary urgency [16,22]. Symptoms are rated on a scale of 0–5 points (0 = no symptoms and 5 = severe symptoms). Hence the maximum score is 35. Based on this self-evaluation of the patient, a total score < 8 corresponds to minimal symptoms, 8–19 to moderate symptoms, and 20–35 to severe symptoms [22]. Clinical success was determined by IPSS-reduction of $\geq 25\%$ and post-procedural IPSS < 17 points as well as QoL-score-reduction of ≥ 1 point or post-procedural QoL-score ≤ 3 points [23]. IPSS-reduction < 25%, IPSS ≥ 18 , QoL-reduction < 1 point or post-procedural QoL-score ≥ 4 points were considered clinical failure [2].

2.9. Statistical analysis

For statistical analysis *BLINDED* (University professor for biostatistics), was consulted. Statistical analyses were performed using BiAS for Windows (version 11.08-03/2018, © epsilon Verlag 1989-2018, Frankfurt am Main, Germany). Normality of data distribution was evaluated for all demographic variables using the Kolmogoroff-Smirnoff-Lilliefors and Chi Square test. Wilcoxon matched paired test was applied for IPSS, QoL, IIEF and PV. For group-comparison, Wilcoxon-Mann-Whitney-U test was used. One and two-sample t-tests were used to test for p-values. Pearson's correlation was applied for PV and IPSS. P-values < 0.05 were considered significant.

3. Results

259 patients, with a mean age of 69 (± 9 , [41–92]) years were analyzed. In 137 patients, PAE was performed using pre-interventional MRA as guidance (Group A). 122 patients underwent PAE without undergoing MRA prior to the procedure (Group B). The median time interval between PAE and follow-up of any kind in our study was 20 weeks in Group A (± 25.64 , min. 12, max. 42) and in Group B 17 weeks (± 24.03 , min. 12, max. 44). MRI Follow Up ≥ 3 months n = 137 (100%/in Group A, Group B n = 122, (100%).

52% of the study population were treated first line with alpha adrenergic antagonists or 5-alpha reductase inhibitors (n = 135; Group A n = 63/Group B n = 72). Post-interventional nausea (n = 4) and vomiting (n = 6) occurred in 10 of 259 patients (4%). A total of 15/259 patients (6%) suffered from pain in the lower abdomen/pelvic region after PAE. 37/259 (14%) of patients reported groin pain and re-

ceived a pressure dressing additionally to the closure device. In 6 of these 37 (16%) cases pseudoaneurysm of the common femoral artery was detected using ultrasound after the intervention in the normal ward.

Mean PSA value in Group A was 0.02 ng/ml (± 0.008 ng/ml) and 0.01 ng/ml (± 0.007 ng/ml) in Group B (*p* greater than 0.05). Pre-interventional mpMRI unveiled Pi-RADS-2 score 1 in 129 of 137 patients in Group A and 120 in Group B, and accordingly n = 8 Pi-RADS-2 score in 2 patients in Group A and n = 2 in Group B.

3.1. Origin of the prostate artery

In 30.62% (n = 79; Group A n = 37/Group B n = 42) the PA arose from inferior vesical artery, in 27.13% (n = 70; Group A n = 39/Group B n = 31) from the internal pudendal artery. In 7.37% (n = 19; Group A n = 7/Group B n = 12) PA originated from obturator artery, in 7.75% (n = 20; Group A n = 11/Group B n = 9) from internal iliac artery and in 1.55% from superior vesical artery (n = 4; Group A n = 3/Group B n = 1). In 25.58% (n = 66; Group A n = 39/Group B n = 27) PA-origin was complex and PA occurred with multiple origins or collateral feeders out of the truncus.

3.2. PAE workflow

16 cases of severe pathological vascular features such as aneurysm n = 5, high grade stenosis (>70%) n = 8, high grade atherosclerosis n = 2, severe elongation n = 1 were detected in MRA. Anatomical variants such as double feeders (n = 1) and atypical origin of prostate artery (n = 66) were reported.

PAE workflow was altered in 12% (n = 16) of cases in Group A (contralateral approach of AFC n = 10, n = 2 transbrachial access, n = 4 two-sided puncture of AFC with ipsilateral embolization) due to MRA findings. Figs. 3 and 4 show two of the mentioned 16 cases in which MRA findings directly influenced and modified PAE workflow in this study.

100–300 μ m particles were used in 41.38% (n = 56) of interventions in Group A, whereas in Group B the usage was 58.62% (n = 72) (*p* < 0.001). 300–500 μ m particles were used in 57.79% of cases (n = 81) in Group A and 42.21% in Group B (n = 50) (*p* < 0.001).

Particle size significantly correlated with reduction in prostate volume (*p* = 0.022). 100–300 μ m particles led to a mean reduction of 11.20 ml [0.97–74.29] whereas 300–500 μ m particles resulted in a mean decrease of –6.85 ml [18.26–39.55] (*p* < 0.001).

Mean amount of used contrast agent during the procedure was 68 ml (± 29 ml [50–120]) in Group A and 113 ml (± 49 ml; [60–200]) in Group B (*p* < 0.001).

3.3. Clinical outcome

Significant IPSS improvements were achieved in both groups. In Group A, the mean reduction was –10.50 points (± 8.24 , [3–27]), whereas the mean reduction in Group B was –7 points (± 8.50 , [8–31]) (*p* < 0.001). In Group A, the mean IPSS baseline was 21 points (± 7.00 , [7–35]) and significantly decreased to 10 points post-intervention (± 6.03) (*p* < 0.001). In Group B, mean IPSS was decreased from 20 points (± 6.44 , [9–35]) to 13.75 points (± 7.83 , [0–35]) (*p* < 0.001) (Fig. 6).

QoL in Group A improved from 4.06 points (± 1.29 , [0–6]) to 13 points (± 1.30 , [0–5]). Mean QoL score in Group B decreased from 4.12 points (± 1.21 , [1–6]) before the treatment to 2.20 points (± 1.50 , [0–6]) after the treatment (see Fig. 6) (*p* = 0.78).

Pre-interventional mean IIEF of Group A was 21.50 points (± 10.15 , [0–30]) and post-interventional 24.02 points (± 10.38 , [0–30]). In Group B, IIEF score started at 23.11 points (± 11.32 , [0–30]) and improved to 24.09 points (± 11.03 , [0–30]).

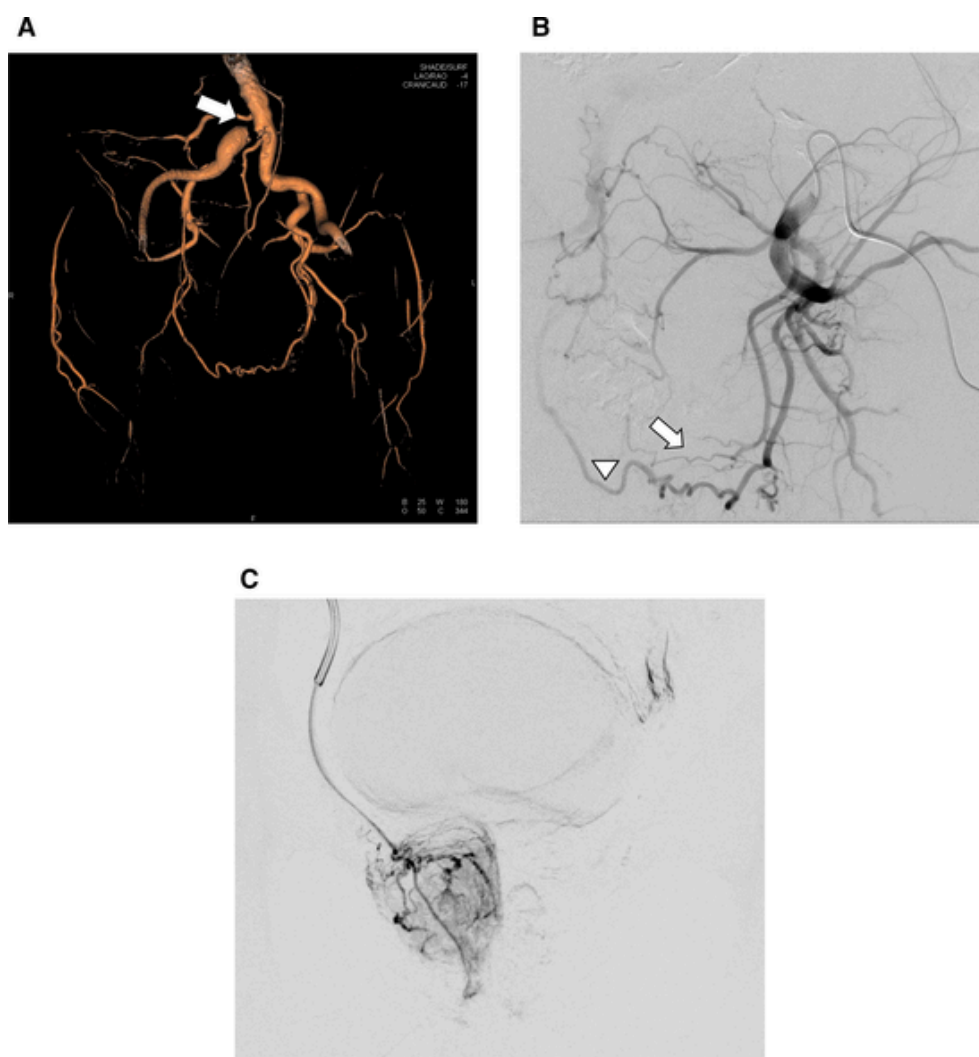


Fig. 3. Case of a 67-year-old patient (Group A) with benign prostatic hyperplasia (BPH) and lower urinary tract symptoms (LUTS). Quality of life (QOL), international index of erectile function (IIEF) and international prostate symptom score (IPSS) scores of 4, 19 and 26 were registered prior to the intervention. Prostatic volume was 67 ml before PAE. In the follow-up, QOL, IIEF and IPSS scores of 2, 19, 14 were reported post-intervention. Prostatic volume was 44 ml 12 weeks after the intervention. Pre-interventional magnetic resonance angiography (MRA) showed subtotal occlusion of the right-sided proximal common iliac artery. Therefore, we prepared both groins for transarterial approach, as it was clear that a crossover maneuver would not be possible. Thus, an ipsilateral retrograde access was chosen for both sides. Fig. 3A shows the pre-interventional reconstructed navigation 3-dimensional-VRT showing subtotal occlusion of the right-sided proximal common iliac artery (AIC)(arrow) also including the necessary information on the angulation of the C-arm with right-anterior oblique and caudal angulation of 4° and 17°. DSA of the internal iliac artery (AII) on the left side, showing total occlusion of the common iliac artery after ipsilateral retrograde access of the left femoral artery with strong collateralization to the contralateral side, to shunt the occlusion of the AIC (Fig. 3B, arrow). The prostatic artery is visible as a branch of the obturator artery (Fig. 3B, arrow head) The parenchyme blush after superselective catheterization of the prostate artery with a microcatheter confirmed the correct catheter position before embolization (Fig. 3C).

No significant difference was found between both groups regarding improvement of IIEF scores ($p = 0.162$) as shown in Fig. 6.

3.4. Prostate volumetry

All initial prostate volumes were greater than 35 ml according to measurements taken from MRI. Benign prostatic hyperplasia (BPH) was present in each patient.

Mean initial prostate volume in Group A was 75.43 ml (± 49.12 , [36.07–344.84]). A mean decrease in prostate volume of -19.92 ml (± 13.22 , [18.26–74.29]) could be achieved in Group A. Mean initial prostate volume in Group B was 71.68 ml (± 31.18 , [35.16–198.31]). In Group B a mean reduction in prostate volume of -16.85 ml (± 9.12 , [7.27–39.55]) was obtained. In 61.40% ($n = 35$) of patients a reduction in prostate volume greater than 10 ml was found in Group A. In

Group B a volumetric reduction of more than 10 ml was accomplished in only 38.60% ($n = 22$).

According to the Wilcoxon-Mann-Whitney-Test, pre-interventional MRA significantly affected prostate volume reduction ($p = 0.032$).

3.5. ADC reduction

Reduction of ADC was considered therapy success indicating precise administration of particles through the PA and consecutive necrosis of the prostatic gland. In Group A, the ADC value at baseline had a mean of $1350.00 \times 10^{-6} \text{ mm}^2/\text{s}$ (± 145.38 , [755.00–1696.00]) and the post PAE ADC value was a mean of $1278.70 \times 10^{-6} \text{ mm}^2/\text{s}$ (± 113.32 , [722.93–1481.40]). In Group B, the ADC value at baseline was a mean of $1271.50 \times 10^{-6} \text{ mm}^2/\text{s}$ (± 135.44 , [756.00–1518.00]) and the post PAE ADC value was a mean of $1241.14 \times 10^{-6} \text{ mm}^2/\text{s}$ (± 148.08 , [593.90–1481.40]). In Group A there was a significantly greater ADC

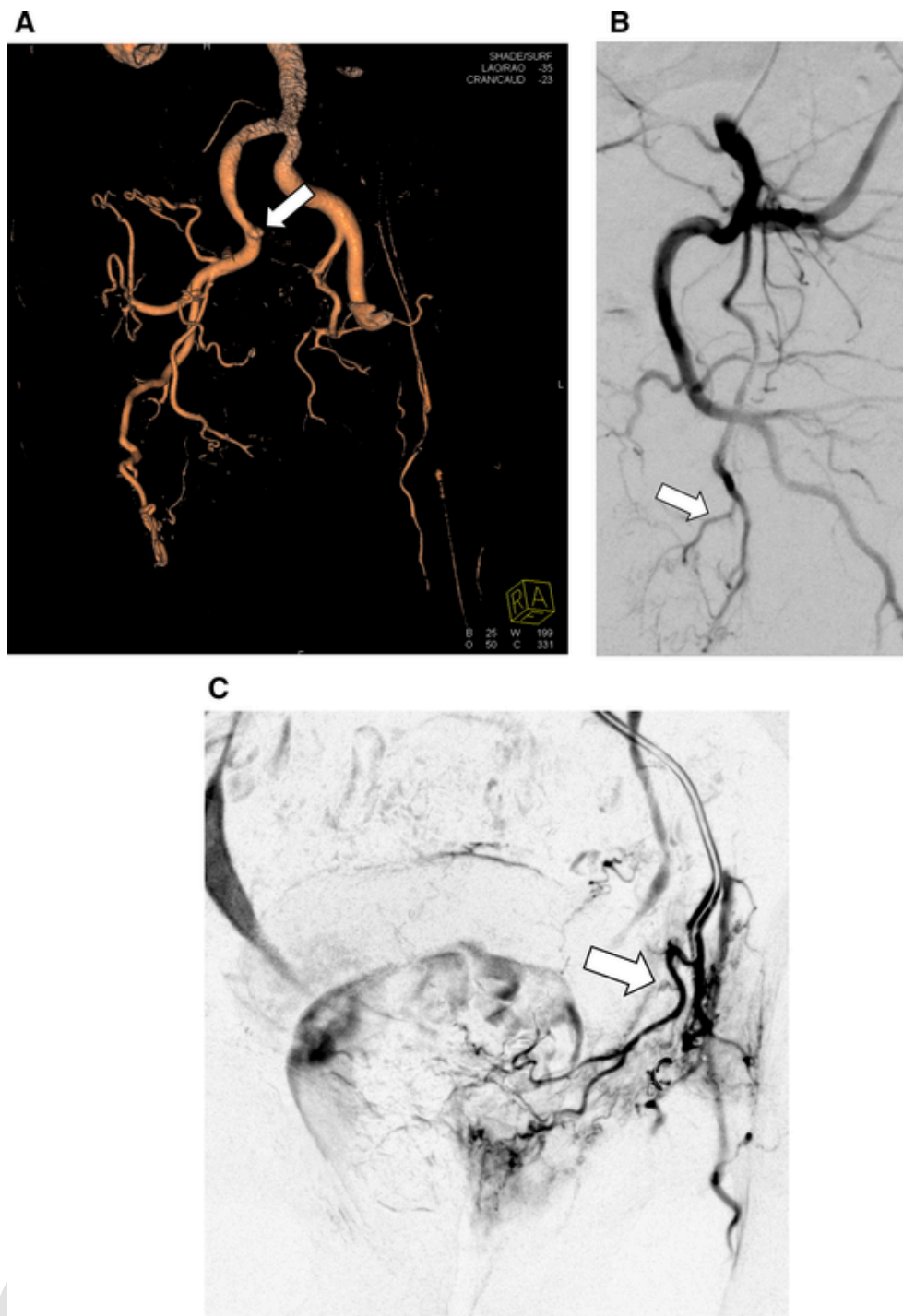


Fig. 4. Case of a 73-year-old patient (Group A) with benign prostatic hyperplasia (BPH) and lower urinary tract symptoms (LUTS). Quality of life (QOL), international index of erectile function (IIEF) and international prostate symptom score (IPSS) scores of 4, 21 and 31 were registered pre-intervention. Prostatic volume was 71 ml before the intervention. In the follow-up, QOL, IIEF and IPSS scores of 2, 20 and 12 were reported post-intervention. Prostatic volume was 44 ml 12 weeks after the intervention. The patient had known high grade stenosis of the common femoral artery on the left side. Pre-interventional magnetic resonance angiography (MRA) depicted a subtotal stenosis of the common femoral artery (Fig. 4A) on the right side. Fig. 4A shows the pre-interventional reconstructed navigation 3-dimensional-VRT in LAO 35°/CAUD 23° angulation. The arrow indicates a subtotal stenosis of the common femoral artery. Thus, a trans-brachial approach was used for catheterization of the prostatic artery (PA) (Fig. 4B and C, arrows) on both sides based on MRA findings in this case.

value reduction ($p = 0.036$ than in Group B (see Fig. 2). In Group A, the mean ADC value reduction was $-77.80 \times 10^{-6} \text{ mm}^2/\text{s}$ (± 111.10 , [178.20–352.20]) whereas in Group B the mean ADC value reduction was $-44.70 \times 10^{-6} \text{ mm}^2/\text{s}$ (± 99.36 , [217.90–362.90]).

3.6. Radiation dose

Cumulative radiation dose measurements showed significantly higher radiation dose for Group B with a mean dose are product (DAP) of $23963.50 \text{ } \mu\text{Gy}\cdot\text{m}^2$ (± 19792.25 , [913.60–108800.00]) compared to

Group A ($5518.54 \mu\text{Gy}\cdot\text{m}^2 \pm 6677.97, [314.71-40679.00]$) (see Fig. 5) ($p < 0.001$).

Mean entrance dose (RP) was significantly lower in Group A with a mean value of $347.15 \text{ mGy} (\pm 415.82, [17.10-2185.00])$ compared to Group B ($1301.70 \text{ mGy} \pm 1181.15, [52.20-6480.39]$) ($p < 0.001$).

In Group A an average of $n = 16 (\pm 8.91, [4-44])$ image series was acquired, and mean fluoroscopy time was $19.35 \text{ min} (\pm 9.01, [4.50-45.80])$.

In Group B an average of $n = 21 (\pm 8.49, [6.00-52.00])$ image series was acquired, and mean fluoroscopy time was $27.45 \text{ min} (\pm 12.54, [6.30-68.40])$ (see Fig. 5).

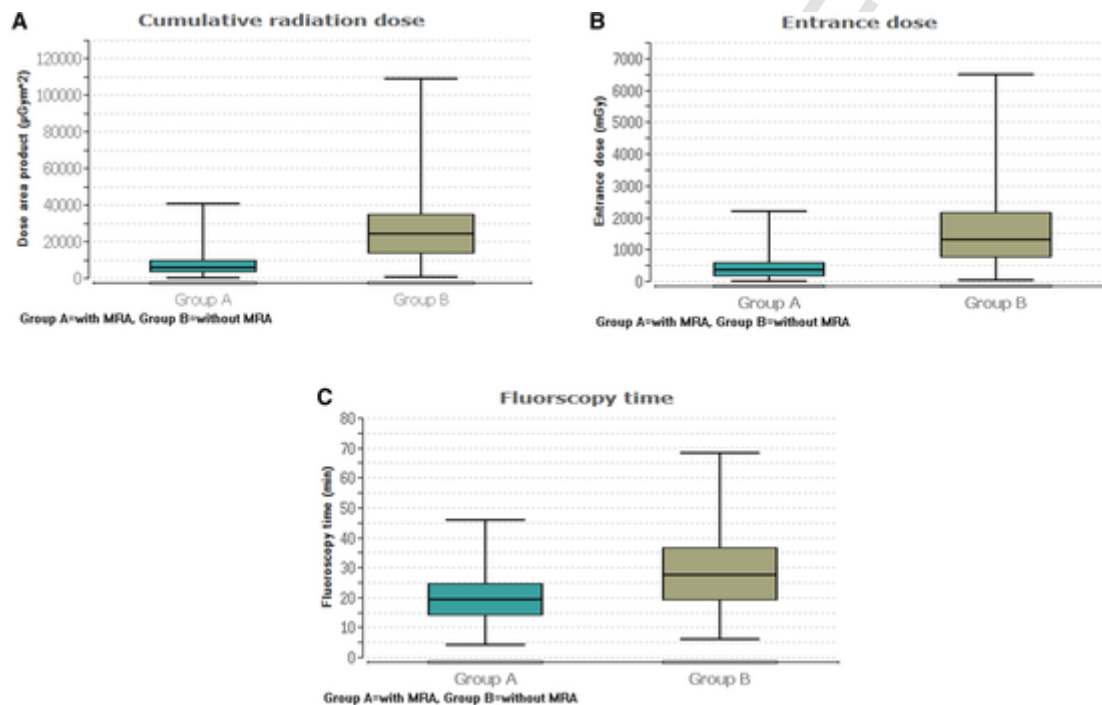


Fig. 5. Boxplots of radiation dose values in Group A and Group B regarding cumulative dose area product (DAP) (Fig. 5A) and entrance dose (RP) (Fig. 5B). In addition, Fig. 5C shows a boxplot displaying fluoroscopy times in Group A and B. All three parameters were significantly different in Group A and B.

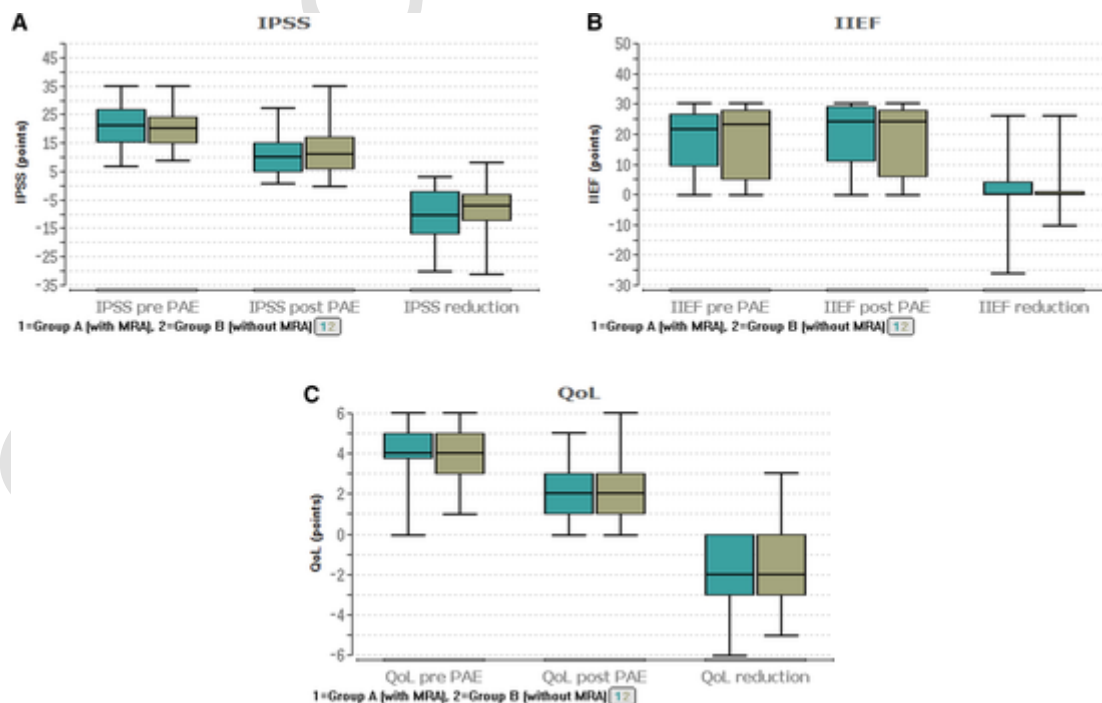


Fig. 6. Boxplots of clinical score values in Group A and B. In our study, international prostate symptom score (IPSS) (Fig. 6A), Quality of life (QOL) (Fig. 6B) and international index of erectile function (IIEF) (Fig. 6C) were used for clinical outcome evaluation. Significant differences were found between Group A and B regarding IPSS. QOL and IIEF did not show any significant differences between results from both groups.

4. Discussion

Pre-interventional MRA resulted in substantial PAE workflow improvements and significantly less radiation exposure as well as shorter fluoroscopy and intervention times.

Prior studies demonstrated high sensitivity of pre-interventional MRA for visualization of the PA [11,12]. In 30% of our patients the PA originated from the inferior vesical artery which is comparable to literature values of 30% to 35% [4,7]. While Zhang et al focused on the potential of MRA for visualization of the PA in a smaller patient population ($n = 100$) [11], we focused on evaluating workflow and clinical outcome. MRA significantly influenced pre-interventional therapy planning. In 16 cases PAE protocol was changed due to findings in MRA. In 10 cases, we approached the PA through left femoral access (standard access is right femoral access). In four cases, an ipsilateral two-sided puncture of the femoral artery was needed to reach the PA due to significant stenosis of the common iliac artery. In two cases, a transbrachial access was needed due to high grade atherosclerosis and aneurysm of the common femoral arteries.

Patients undergoing MRA prior to PAE received more frequently bigger embolization particles compared to patients without pre-interventional MRA. This may be an incidental finding, as the choice of particle size was depending on the visibility/presence of relevant collaterals and the correct target catheter position without any risk of non-target embolization. In case of visible collaterals and a risk of non-target embolization, we chose the bigger particle size in order to avoid non-target embolization as much as possible. In case of visual absence of relevant collaterals, we used the smaller particle size. This was resulting in a small difference in particle size usage between both patient groups (100–300 μm : 41.38% ($n = 56$) of interventions in Group A, vs. 58.62% in Group B; $p < 0.05$). In this context, no significant correlation between particle size and efficacy of volume reduction has been found in literature [24,25].

Our baseline mean initial prostate volume in Group A was 75.43 ml (± 49.12 , [36.07–344.84]) versus 71.68 ml in Group B (± 31.18 , [35.16–198.31]) ($p = 0.21$). PV-reduction was observed to be higher in the group receiving pre-interventional imaging, compared to PAE without pre-interventional MRA (–19.92 ml in Group A vs –16.85 ml in Group B). This is controversial to the findings of Zhang et. al., who did not report any differences in prostatic volume reduction (–41 ml in both groups). Our results may be an incidental finding, which might be explained by the fact that in Group A the smaller particles were used more frequently. Also, the overall prostatic volume and volume reduction does not correlate with the severity and improvement of LUTS in literature [26]. Compared to our baseline PV, other studies conducted examining the impact of PV on the severity of LUTS started with prostatic volumes of ~35 ml [27]. Therefore, the higher volume reduction in Group A could be caused by the patient population exclusively.

ADC analysis revealed a significantly higher diffusion restriction in ADC values in patients undergoing MRA prior PAE, indicating that induced ischemia of the target parenchyma was substantially higher in Group A.

Patients undergoing MRA prior to PAE received 40% less contrast agent (68 ml \pm 29 ml vs 113 ml \pm 49 ml) during intervention, showing potential benefits for patients with impaired renal function. Fluoroscopy times were significantly shorter using MRA (19.35 min \pm 9.01, [4.50–45.80]) compared to the group without MRA (27.45 min \pm 12.54, [6.30–68.40]). These results are in accordance with Zhang and Kobe et al. [8,11] who reported 13.8 \pm 2.7 min vs 28.5 \pm 8 min and 33.2 \pm 15.1 min showing shorter intervention times using MRA.

Regarding clinical outcome, patients undergoing pre-interventional MRA before PAE showed a significantly higher reduction of IPSS (–10.50 \pm 8.24 points vs –7 \pm 8.50 points; $p < 0.001$). QOL and erectile function scores demonstrated no significant differences be-

tween both patient groups ($p > 0.05$). Overall, the higher IPSS score improvement in Group A could not be directly correlated to acquisition of pre-interventional MRA and will most likely be linked to the individual therapy response of the patients in this cohort. As the clinical scores in both groups improved significantly after PAE, the clinical success was verified for both groups regardless of the pre-interventional imaging.

MRA decreases the overall radiation dose in the context of PAE in contrast to well established angiography modalities, such as intraprocedural CBCT and pre-interventional MDCT. In recent literature, CBCT-based radiation dose was reported with a range from 310.5 \pm 148.7 Gy·cm up to 454 \pm 171 Gy·cm², which represents up to 76% of the entire radiation exposure of the intervention [8,28]. In comparison, pre-interventional CTA resulted in additional mean radiation dose of 36.6 \pm 7.9 mGy, a dose length product of 756.6 \pm 168.8 mGy·cm², and effective dose of 11.3 \pm 2.5 mSv [8]. Thus, commonly reported radiation induced complications, such as skin erythema, hair loss and stochastic cancer risk [6], may be effectively decreased by implementation of MRA in context of PAE. With a mean total DAP of 239,6 Gy·cm² we were nearly 47% lower compared to DAP values reported in recent literature of 450.7 Gy·cm² (Andrade et al.) [5, 10,28]. Our reported mean RP was 347.15 mGy (\pm 415.82) for Group A and 1301.70 mGy (\pm 1181.15) in Group B, which was significantly lower compared to literature values of 2674.2 mGy [10].

In our opinion, pre-interventional imaging is highly recommended in all patients undergoing PAE to contain complications, with MRA being preferably used, if available to avoid additional radiation exposure.

There are several limitations to address. First, this was a retrospective single center study, including patients undergoing PAE in a limited time interval based on one intervention protocol. Results regarding workflow optimization are dependent on the standard protocol and could be different for other intervention protocols. Our follow-up time interval was limited due to missing patient feedback after 6 months (63% of patients with complete clinical follow-up data and MRI. We recommend a multi-center prospective blinded randomized controlled trial to verify our data.

5. Conclusion

In conclusion, our study demonstrated that pre-interventional MRA results in substantial PAE workflow optimization, while significantly decreasing radiation exposure and intervention time. As pre-interventional imaging and planning plays a key role for the success of PAE, we therefore recommend implementation of MRA to PAE workflow.

Compliance with ethical standards

Guarantor: The scientific guarantor of this publication is Prof. Dr. Thomas J. Vogl (Department of Diagnostic and Interventional Radiology, University Hospital Frankfurt).

Statistics and Biometry: No complex statistical methods were necessary for this paper.

Informed Consent: Only if the study is on human subjects: Written informed consent was waived by the Institutional Review Board.

Ethical Approval: Institutional Review Board approval was obtained.

Methodology:

- retrospective
- comparative study
- performed at one institution

Funding

The authors state that this work has not received any funding.

CRediT authorship contribution statement

Thomas J. Vogla: Conceptualization, Writing – original draft. **Christian Booz:** Methodology, Writing – review & editing. **Vitali Koch:** Investigation, Data curation. **Nour Eldin A. Nour-Eldin:** Writing – review & editing. **Emad H. Emara:** Writing – review & editing. **Felix Chun:** Conceptualization, Validation. **Shirin El Nemr:** Data curation, Writing – original draft. **Leona S. Alizadeh:** Data curation, Writing – original draft, Conceptualization, Validation.

Declaration of Competing Interest

The authors declare the following financial interests/personal relationships which may be considered as potential competing interests: [The authors of this manuscript declare relationships with the following companies: C.B. received speaking fees from Siemens Healthineers. The other authors have no potential conflict of interest to disclose.]

References

- [1] F.C. Carnevale, A.M. Moreira, A.M. de Assis, A.A. Antunes, V. Cristina de Paula Rodrigues, M. Srougi, G.G. Cerri, Prostatic Artery Embolization for the Treatment of Lower Urinary Tract Symptoms Due to Benign Prostatic Hyperplasia: 10 Years' Experience, *Radiology* 296 (2) (2020) 444–451.
- [2] J.M. Pisco, L.C. Pinheiro, T. Bilhim, M. Duarte, J.R. Mendes, A.G. Oliveira, Prostatic Arterial Embolization to Treat Benign Prostatic Hyperplasia, *J. Vasc. Interv. Radiol.* 22 (2011) 11–19, <https://doi.org/10.1016/j.jvir.2010.09.030>.
- [3] A.C. Picel, T.-C. Hsieh, R.M. Shapiro, A.M. Vezeridis, A.J. Isaacson, Prostatic Artery Embolization for Benign Prostatic Hyperplasia: Patient Evaluation, Anatomy, and Technique for Successful Treatment, *RadioGraphics*. 39 (2019) 1526–1548, <https://doi.org/10.1148/rg.2019180195>.
- [4] T. Bilhim, H.R. Tinto, L. Fernandes, J. Martins Pisco, Radiological Anatomy of Prostatic Arteries, *Techniques Vasc. Int. Radiol.* 15 (4) (2012) 276–285.
- [5] G. Andrade, H.J. Khoury, W.J. Garzón, F. Dubourcq, M.F. Bredow, L.M. Monsignore, D.G. Abud, Radiation Exposure of Patients and Interventional Radiologists during Prostatic Artery Embolization: A Prospective Single-Operator Study, *J. Vasc. Interv. Radiol.* 28 (2017) 517–521, <https://doi.org/10.1016/j.jvir.2017.01.005>.
- [6] A. Laborda, A.M. De Assis, I. Ioakeim, M. Sánchez-Ballestín, F.C. Carnevale, M.A. De Gregorio, Radiodermatitis After Prostatic Artery Embolization: Case Report and Review of the Literature, *Cardiovasc. Intervent. Radiol.* 38 (2015) 755–759, <https://doi.org/10.1007/s00270-015-1083-6>.
- [7] F.C. Carnevale, G.R. Soares, A.M. de Assis, A.M. Moreira, S.H. Harward, G.G. Cerri, Anatomical Variants in Prostate Artery Embolization: A Pictorial Essay, *Cardiovasc. Intervent. Radiol.* 40 (2017) 1321–1337, <https://doi.org/10.1007/s00270-017-1687-0>.
- [8] A. Kobe, G. Puipe, E. Klotz, H. Alkadhi, T. Pfammatter, Computed Tomography for 4-Dimensional Angiography and Perfusion Imaging of the Prostate for Embolization Planning of Benign Prostatic Hyperplasia, *Invest. Radiol.* 54 (2019) 661–668, <https://doi.org/10.1097/RLI.0000000000000582>.
- [9] M.Q. Wang, F. Duan, K. Yuan, G.D. Zhang, J. Yan, Y. Wang, Benign Prostatic Hyperplasia: Cone-Beam CT in Conjunction with DSA for Identifying Prostatic Arterial Anatomy, *Radiology* 282 (2017) 271–280, <https://doi.org/10.1148/radiol.2016152415>.
- [10] W.J. Garzón, G. Andrade, F. Dubourcq, D.G. Abud, M. Bredow, H.J. Khoury, R. Kramer, Prostatic artery embolization: radiation exposure to patients and staff, *J. Radiol. Prot.* 36 (2016) 246–254, <https://doi.org/10.1088/0952-4746/36/2/246>.
- [11] J.L. Zhang, M.Q. Wang, Y.G. Shen, H.Y. Ye, K. Yuan, H.N. Xin, H.T. Zhang, J.X. Fu, J.Y. Yan, Y. Wang, Effectiveness of Contrast-enhanced MR Angiography for Visualization of the Prostatic Artery prior to Prostatic Arterial Embolization, *Radiology* 291 (2019) 370–378, <https://doi.org/10.1148/radiol.2019181524>.
- [12] A.Y. Kim, D.H. Field, D. DeMulder, J. Spies, P. Krishnan, Utility of MR Angiography in the Identification of Prostatic Artery Origin Prior to Prostatic Artery Embolization, *J. Vasc. Interv. Radiol.* 29 (2018) 307–310.e1, <https://doi.org/10.1016/j.jvir.2017.11.001>.
- [13] J.N. Thai, H.A. Narayanan, A.K. George, M.M. Siddiqui, P. Shah, F.V. Mertan, M.J. Merino, P.A. Pinto, P.L. Choyke, B.J. Wood, B. Turkbey, Validation of PI-RADS Version 2 in Transition Zone Lesions for the Detection of Prostate Cancer, *Radiology* 288 (2018) 485–491, <https://doi.org/10.1148/radiol.2018170425>.
- [14] B. Turkbey, P.A. Pinto, H. Mani, M. Bernardo, Y. Pang, Y.L. McKinney, K. Khurana, G.C. Ravizzini, P.S. Albert, M.J. Merino, P.L. Choyke, Prostate Cancer: Value of Multiparametric MR Imaging at 3 T for Detection—Histopathologic Correlation, *Radiology* 255 (2010) 89–99, <https://doi.org/10.1148/radiol.09090475>.
- [15] A.P. Berger, M. Deibl, A. Strasak, J. Bektic, A.E. Pelzer, H. Klocker, H. Steiner, G. Fritsche, G. Bartsch, W. Horninger, Large-Scale Study of Clinical Impact of PSA Velocity: Long-Term PSA Kinetics as Method of Differentiating Men with from Those without Prostate Cancer, *Urology*. 69 (2007) 134–138, <https://doi.org/10.1016/j.urol.2006.09.018>.
- [16] C. Gratzke, A. Bachmann, A. Descazeaud, M.J. Drake, S. Madersbacher, C. Mamoulakis, M. Oelke, K.A.O. Tikkinen, S. Gravas, EAU Guidelines on the Assessment of Non-neurogenic Male Lower Urinary Tract Symptoms including Benign Prostatic Obstruction, *Eur. Urol.* 67 (2015) 1099–1109, <https://doi.org/10.1016/j.eururo.2014.12.038>.
- [17] A.C. Picel, T.-C. Hsieh, R.M. Shapiro, A.M. Vezeridis, A.J. Isaacson, Prostatic artery embolization for benign prostatic hyperplasia: Patient evaluation, anatomy, and technique for successful treatment, *Radiographics*. 39 (5) (2019) 1526–1548.
- [18] A.M. de Assis, A.M. Moreira, V.C. de Paula Rodrigues, S.H. Harward, A.A. Antunes, M. Srougi, F.C. Carnevale, Pelvic Arterial Anatomy Relevant to Prostatic Artery Embolisation and Proposal for Angiographic Classification, *Cardiovasc. Intervent. Radiol.* 38 (4) (2015) 855–861.
- [19] J. Sosna, N.M. Rofsky, S.M. Gaston, W.C. DeWolf, R.E. Lenkinski, Determinations of prostate volume at 3-tesla using an external phased array coil, *Acad. Radiol.* 10 (2003) 846–853, [https://doi.org/10.1016/S1076-6332\(03\)00015-1](https://doi.org/10.1016/S1076-6332(03)00015-1).
- [20] F.C. Carnevale, A.M. Moreira, A.A. Antunes, The “PerFecTED Technique”: Proximal Embolization First, Then Embolize Distal for Benign Prostatic Hyperplasia, *Cardiovasc. Intervent. Radiol.* 37 (2014) 1602–1605, <https://doi.org/10.1007/s00270-014-0908-z>.
- [21] R.C. Rosen, A. Riley, G. Wagner, I.H. Osterloh, J. Kirkpatrick, A. Mishra, The international index of erectile function (IIEF): a multidimensional scale for assessment of erectile dysfunction, *Urology*. 49 (1997) 822–830, [https://doi.org/10.1016/S0090-4295\(97\)00238-0](https://doi.org/10.1016/S0090-4295(97)00238-0).
- [22] M.J. Barry, F.J. Fowler, M.P. O'leary, R.C. Bruskewitz, H.L. Holtgrewe, W.K. Mebust, A.T.K. Cockett, Measurement Committee of the American Urological Association, The American Urological Association Symptom Index for Benign Prostatic Hyperplasia, *J. Urol.* 197 (2S) (2017), <https://doi.org/10.1016/j.juro.2016.10.071>.
- [23] D. Maclean, M. Harris, T. Drake, B. Maher, S. Modi, J. Dyer, B. Somani, N. Hacking, T. Bryant, Factors Predicting a Good Symptomatic Outcome After Prostate Artery Embolisation (PAE), *Cardiovasc. Intervent. Radiol.* 41 (2018) 1152–1159, <https://doi.org/10.1007/s00270-018-1912-5>.
- [24] T. Bilhim, J. Pisco, L. Campos Pinheiro, H. Rio Tinto, L. Fernandes, J.A. Pereira, M. Duarte, A.G. Oliveira, Does Polyvinyl Alcohol Particle Size Change the Outcome of Prostatic Arterial Embolization for Benign Prostatic Hyperplasia? Results from a Single-Center Randomized Prospective Study, *J. Vasc. Interv. Radiol.* 24 (2013) 1595–1602.e1, <https://doi.org/10.1016/j.jvir.2013.06.003>.
- [25] R. Geervarghese, J. Harding, N. Parsons, C. Hutchinson, C. Parsons, The relationship of embolic particle size to patient outcomes in prostate artery embolisation for benign prostatic hyperplasia: a systematic review and meta-regression, *Clin. Radiol.* 75 (2020) 366–374, <https://doi.org/10.1016/j.crad.2019.12.019>.
- [26] M. Franciosi, W.J. Koff, E.L. Rhoden, Correlation between the total volume, transitional zone volume of the prostate, transitional prostate zone index and lower urinary tract symptoms (LUTS), *Int. Urol. Nephrol.* 39 (2007) 871–877, <https://doi.org/10.1007/s11255-006-9148-8>.
- [27] Y.B. Jeong, K.S. Kwon, S.D. Kim, H.J. Kim, Effect of Discontinuation of 5 α -Reductase Inhibitors on Prostate Volume and Symptoms in Men With BPH: A Prospective Study, *Urology*. 73 (2009) 802–806, <https://doi.org/10.1016/j.jurology.2008.10.046>.
- [28] M. Chiaradia, A. Radaelli, A. Campeggi, M. Bouanane, A. De La Taille, H. Kobeiter, Automatic Three-Dimensional Detection of Prostatic Arteries Using Cone-Beam CT during Prostatic Arterial Embolization, *J. Vasc. Interv. Radiol.* 26 (2015) 413–417, <https://doi.org/10.1016/j.jvir.2014.11.009>.